Neutron Yield of Thermo Scientific P385 D-T Neutron Generator *vs.* Current and Voltage

Jihye Jeon, Robert J. Goldston, and Erik P. Gilson

***Abstract*—The Thermo Scientific P385 Neutron Generator is a compact neutron source, producing 14 MeV neutrons through the deuterium-tritium (DT) fusion reaction. It is important to measure and understand the dependence of the neutron production rate on the accelerator current and voltage. In this study we evaluated neutron production with an absolutely calibrated liquid scintillator neutron spectrometer (BTI N-Probe), an absolutely calibrated He-3 detector surrounded by HDPE shells (Detec Nested Neutron Spectrometer, NNS), and two uncalibrated ZnS fast neutron scintillators (EJ-410), for both A3082 and A3083 sealed tubes. We also modeled the neutron yield using the TRIM code, which calculates the trajectory and the energy loss of deuterons and tritons within the target. Experimental results showed an essentially linear dependence on beam current, as expected. A 3.59 $\pm$0.08 power law dependence on the operating voltage was measured, in effective agreement with the modeled value of 3.5. A series of absolute NNS and N-Probe measurements, matched against MCNP calculations, showed that the A3083 and A3082 tubes provide a maximum neutron yield of 8.2×10^8 n/s and 4.7×10^8 n/s respectively, with estimated uncertainty of $\pm$10%. We showed, through modeling, that tritium decay is not a significant consideration for tubes, such as these, with lifetimes of less than 10 years.**

***Index Terms*—accelerator-based neutron source, DT neutron generator, P385 neutron generator**

I. Introduction

THE Thermo Scientific P385 Neutron Generator is a compact neutron source with a specified maximum neutron yield of 5×10^8 neutrons/s [1]. The P385 creates 14 MeV neutrons by the deuteron-triton (DT) fusion reaction. In our laboratory, we are exploring its use in neutron radiography for arms control [2]. The neutron yield of the generator is controlled by the operating current and voltage of the accelerator. The P385 with DT neutron tube model A3082 is specified to have a yield of 5×10^8 n/s at its maximum current of 70 μA and maximum voltage of 130 kV. The A3083 tube, provided in a separate accelerator head, is specified to produce 8×10^8 n/s at its maximum current of 90 μA and maximum voltage of 140 kV. To better characterize the source for future applications, it is important to understand the dependence of neutron production rate on the accelerator current and voltage.

This work was supported by the U.S. Department of Energy under contract number DE-AC02-09CH11466. The United States Government retains a non-exclusive, paid-up, irrevocable, world-wide license to publish or reproduce the published form of this manuscript, or allow others to do so, for United States Government purposes.

Jihye Jeon is with Princeton University, Princeton, NJ 08542 USA (e-mail: jihyej@princeton.edu).

Robert J. Goldston is with Princeton University and the Princeton Plasma Physics Laboratory, Princeton, NJ 08540 USA (e-mail: goldston@pppl.gov).

Erik P. Gilson is with the Princeton Plasma Physics Laboratory, Princeton, NJ 08540 USA (e-mail: egilson@pppl.gov).

The ASME standard test method for measuring neutron fluence from a 14 MeV neutron generator involves using threshold activation reactions [3], [4]. This technique requires exposing metal foils to neutrons and then measuring the gamma-rays emitted due to neutron activation. In this study, we instead utilized available detectors with traceable calibrations to determine the absolute neutron yield to an estimated accuracy of $\pm$10%.

In a study using another model of DT generator, GENIE 16, the authors determined the voltage dependence, which was found to have a power law of 3.2, based on 11 different combinations of high voltage and current [5]. The vendor of the GENIE 16, SODERN, estimates the neutron flux to be proportional to the current and to follow a power law of 3.5–3.7 with respect to the voltage from 60 kV to 120 kV (GENIE16 User Manual). On the other hand, the Thermo Scientific P385 Operation Manual states that the neutron output depends linearly on the current and depends on the high voltage with the power law relationship of 1.5 [6]. We were told by Thermo Scientific that this was based on their earlier activation foil measurements, but that actual operational experience could be different.

This paper provides modeling and experimental measurements of the scaling of the neutron production rate of the P385 DT neutron generator with beam current and voltage. Furthermore, it validates the absolute source rate of the A3083 and A3082 tubes. Finally, it examines the effect of tritium decay on performance. In this study, we used the continuous mode of operation of the neutron generator exclusively, without pulsing the beam current, as our future application will involve long-duration radiographic and fission neutron measurements.

II. Neutron Yield Calculation

We wrote a simple Python code to calculate the neutron yield as a function of incident beam energy, based on TRIM calcutions of ion transport in the target.

For our conditions of very low fusion fraction per spatial step, the fraction of incoming ions that undergoes fusion is given by

$$f = n_t \sum_i \Delta l_i \ \sigma_{\mathrm{fus},i} \tag{1}$$

where the i denotes individual steps by the beam ions within the target material between its initial high energy and final low energy. n_t is the target density. $\Delta l_i = \sqrt{(\Delta x_i)^2 + (\Delta y_i)^2 + (\Delta z_i)^2}$ is the length of the i'th step, and $\sigma_{\mathrm{fus},i}$ is the fusion cross-section for the specified beam and target species, using the beam energy at the i'th step.

We calculated Δl using the TRIM code (the Transport of Ions in Matter) [8], which is a Monte Carlo program capable of calculating the 3D distribution of energetic ions in the target. TRIM provided the trajectories of 10,000 deuterons and tritons, including both longitudinal and transverse straggling, at energy intervals of 100 eV. Then we calculated Δl between steps. We used the ENDF/B-VIII.0 library to interpolate the fusion cross section, $\sigma_{\mathrm{fus},i}$, at the corresponding energy of the beam species, assuming the target species was at rest. We calculated the fusion rate of the individual 10,000 ions with the same initial energy using the equation and then acquired the average value.

Based on communication with Thermo Scientific [7] about the estimated properties of the target, we assumed that the target is 1.5 μm thick titanium metal loaded with 1.85 hydrogenic atoms per titanium atom, so that we would have $n_T = n_D = 0.925 n_{Ti}$ where n_T, n_D and n_{Ti} are the number density of tritium, deuterium and titanium atoms in the target. We eliminated ions that traveled more than 1.5 μm into the titanium metal, but in practice almost all of the yield occurred before the particles reached 0.5 μm.

Thermo Scientific [7] estimated the beam to be 90% diatomic (DT^+, TT^+, DD^+) and 10% monatomic (D^+, T^+). Any triatomic component, e.g., DDT^+, was considered to be negligible. The atomic (or monatomic) and molecular beam give us different neutron production yields. Since even with the same acceleration energy, for example, a deuterium in a DD^+ molecular beam will have half energy of a deuteron in monatomic D^+ beam, and in the relevant energy range two deuterons at half energy produce fewer neutrons than one deuteron at full energy. The mix of D and T was given as 50:50 at the time of production of the tubes.

In a monatomic beam, we expect the D^+ or T^+ to have energy eV_{acc} where V_{acc} is the full accelerator voltage. Thus the maximum energy that either species can have in our experiments is $eV_{\mathrm{acc,max}}$, where $eV_{\mathrm{acc,max}}$ is the maximum applied accelerator voltage. In a diatomic beam both nuclei are moving at the same velocity. Thus, in a diatomic beam, the nuclei share the energy proportional to their atomic mass, as shown in Table I.

We have a beam electrical current of I_{acc}, but we need "currents" of nuclei. We assume that D and T are evenly mixed in the beam (and target) and then we have that the full energy atomic D and T beams are equal so D^+ and T^+ ions take half of 10% of total current. When it comes to diatomic beams, simple combinatorial arguments indicate that 1/2 of 90% of total current should be delivered in the form of DT^+ and 1/4 in each of the forms DD^+ and TT^+. The energy and current of each atom in the beam is summarized in Table I.

In the calculation, this breakdown on the current of nuclei was taken into account as a weighting factor for the linear combination of each atomic and molecular beam.

TABLE I
ENERGY AND CURRENT OF BEAM PARTICLES WITH THE ACCELERATOR VOLTAGE V_{acc} AND CURRENT I_{acc}.

Ion	Energy	Current
10% atomic beam		
D^+	eV_{acc}	$0.05 I_{\mathrm{acc}}$
T^+	eV_{acc}	$0.05 I_{\mathrm{acc}}$
90% molecular beam		
DD^+	$0.5eV_{\mathrm{acc}}$ (D), $0.5eV_{\mathrm{acc}}$ (D)	$0.225 I_{\mathrm{acc}}$ (D), $0.225 I_{\mathrm{acc}}$ (D)
TT^+	$0.5eV_{\mathrm{acc}}$ (T), $0.5eV_{\mathrm{acc}}$ (T)	$0.225 I_{\mathrm{acc}}$ (T), $0.225 I_{\mathrm{acc}}$ (T)
DT^+	$0.4eV_{\mathrm{acc}}$ (D), $0.6eV_{\mathrm{acc}}$ (T)	$0.45 I_{\mathrm{acc}}$ (D), $0.45 I_{\mathrm{acc}}$ (T)

III. EXPERIMENTS

We conducted a series of experiments to measure the dependence of neutron production on the intensity of neutron beam. The absolutely calibrated neutron detectors are a BTI N-Probe (N-Probe, Bubble Technology Industries, Inc.) and a Detec Nested Neutron Spectrometer (NNS, Detec, Inc.) as shown in Figure 1. The N-Probe is effective at unfolding neutrons into a spectrum from 20 MeV down to 800 keV using a NE-213 liquid scintillator, while the NNS is well-suited for unfolding neutrons from 20 MeV down to 1 meV using a He-3 counter surrounded by HDPE cylinders of differing thickness.

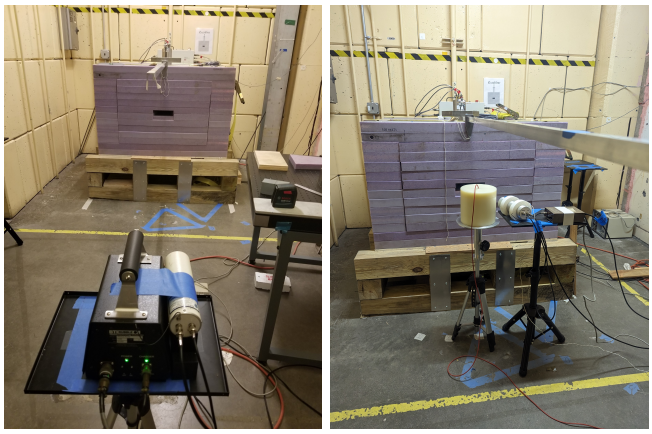

Fig. 1. Experimental configuration. P385 neutron source is surrounded by a carbon steel and borated polyethylene collimator [9]. A neutron exit aperture that has a tapered shape in the horizontal plane is created in the steel cylinder and polyethylene block with an opening angle of 17.5 degrees and a height of 2″. The left figure shows the BTI N-Probe and a EJ-410 detector at 3 m distance. The right figure shows the Detec NNS and an EJ-410 detector placed at 1 m distance from the source. In both configurations, another EJ-410 detector is on the floor under the P385 and the collimator, covered by a layer of 2″-thick lead bricks, which is not shown in the picture. Between the P385 and the EJ-410 on the floor, there is a cylindrical cavity in the collimator and moderator, directed towards this detector. Based on MCNP calculations, the collimator changes the energetic (above 6 MeV) neutron flux at the center of the beamline by less than 10% compared with an ideal, open beam, while it strongly reduces the energetic neutrons available for scattering in the room. The aperture of the collimator represents 0.2% of 4π, and the fraction of neutrons above 6 MeV penetrating the shielding at an angle of 25 degrees off the beam is 0.5%.

The BTI N-Probe, coupled with BTI MICROSPEC analyzer, provides a neutron spectrum by spectral unfolding [11]. The BTI N-Probe was used to count neutrons for current dependence measurements and provide a neutron spectrum for absolute source rate analysis. The N-Probe was placed 3 m away from the target of the P385 where 14 MeV neutrons are generated.

The Detec Nested Neutron Spectrometer, NNS, consists of seven high density polyethylene (HDPE) cylindrical shells and a ^{3}He proportional counter. The HDPE shells are assembled in

a nested fashion so that eight independent measurements can be made, from the bare ^{3}He detector to all the seven shells. For the case of a uniform neutron flux, this permits determination of a neutron spectrum by unfolding [12]. However, the projection of the collimated beam at 1 m is ∼8.3 cm high and the tallest (and thickest) shell is xyz cm. Therefore, we deemed that for this collimated source it is not necessarily appropriate to use the built-in response function of the NNS. For voltage dependence measurements, the NNS was left at 1 m distance from the source with six HDPE shells for all operating voltages, since this setup gives us the most neutron counts among the eight measurements. For absolute source rate experiments, we measured neutrons with the NNS with all 7 shells and then subsequently removed one shell around the detector and counted neutrons for each configuration, as in the conventional NNS measurements, except not using the unfolding process, but comparing to MCNP calculations.

For both the N-Probe and the NNS, a 2″ ZnS fast neutron detector (EJ-410, Eljen Technology, Inc.) was always placed next to N-Probe or NNS to provide a parallel relative measurement for scaling studies.

IV. Results

A. Current and voltage dependence

Figure 2 shows the current dependence of the A3082 neutron emission rate at the operating voltage of 130 kV. When fitted with a power law, the neutron counts from the N-Probe and two EJ-410 fast neutron detectors had scaling exponents close to unity with the P385 tube current over the working range 40–70 μA. The EJ-410 detector at 3 m showed the most deviation from linearity with a power of 1.09 ($\pm$0.05) and the one under the source presented the most linearity with a power of 1.03 ($\pm$0.03).

With regard to voltage dependence at a current of 70 μA, we found that the neutron flux scales like the 3.50–3.64 power of the tube voltage over the working range 60–130 kV for the tube A3082 and 3.58–3.71 power over 60–140 kV for the A3083 as shown in Figure 3. These power law exponents match with the GENIE 16 user manual (power law exponent of 3.5–3.7) and an unpublished study (power law exponent of 3.61 – 3.74) [15]. That study used a Thermo Scientific MP 320 Neutron Generator and measured the neutron yield under the current of 40 – 60 μA and the voltage of 50 – 90 kV. We were able to fit the measured curve vs. voltage by a power law of 3.61 – 3.74. The TRIM calculation is in good agreement with our measurements, showing the power of 3.53 and 3.48 for the A3082 and A3083, respectively, where the small difference is due to the range of voltages tested. The EJ-410 scintillator under the source, covered with a lead block, and the NNS showed close power scaling. Their power exponents only differ by 0.28% for A3082 and 0.14% for A3083.

Overall, we conclude that the scaling with beam current is essentially linear, and the scaling with beam voltage has a power law of 3.59 $\pm$0.08. Both of these are effectively consistent with our first-principles modeling.

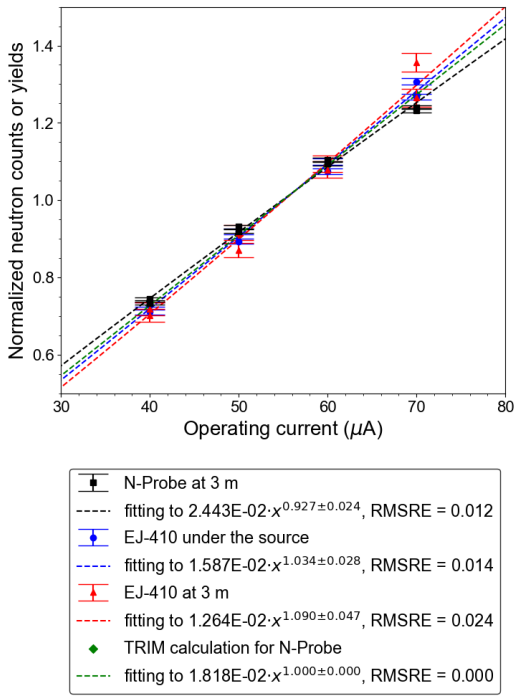

Fig. 2. Theoretical and experimental results on current scanning of P385 A3082. The A3082 tube was operated at its maximum voltage of 130 kV. Instead of using the neutron flux from the unfolded spectrum of the N-Probe, we used the pulse height spectrum which has less scatter. The energy range of 4–10 MeV is chosen where it shows a counting plateau in the integral pulse height spectra, providing maximum stability over long periods of time [14]. The neutron counts from measurements and the yield from TRIM calculations were normalized by their respective means for comparison. The root mean squared relative error (RMSRE) for each fitting is noted.

B. Absolute source rate

We measured the absolute source rate at the maximum operating settings of the A3082 and A3083. First, the full set of NNS measurements of the A3083 tube was performed at its maximum setting, current of 90 μA and voltage of 140 kV. The NNS has been calibrated with an AmBe standard source of the Ionizing Radiation Standards Laboratory at the National research Council of Canada (IRS-NRC). The detector calibration tests were conducted in a low-scatter facility and the neutron output of the AmBe source, with a 2% uncertainty, is traceable to National Institute of Standards and Technology (NIST) [12]. Considering the unfolding process, an additional uncertainty of 2–3% may be assumed, resulting in an estimated total uncertainty of 5% [13]. A Monte Carlo calculation by MCNP6 [16] was conducted for each shell configuration, to determine the corresponding absolute emission. Weighting eight measurements by their neutron counts, the maximum source rate of the A3083 was found to be 8.2×10^8 n/s. Figure 4 compares the neutron counts from the eight measurements from experiment and calculation after taking into account the estimated A3083 source rate. The error in the fit between the measurement and the MCNP modeling, which is dominated by high energy neutrons with the largest number of shells, and lower energy neutrons at the lower number of shells, is in the range of $\pm$5%. Thus we estimate the uncertainty in the overall absolute measurement to be $\pm$10%.

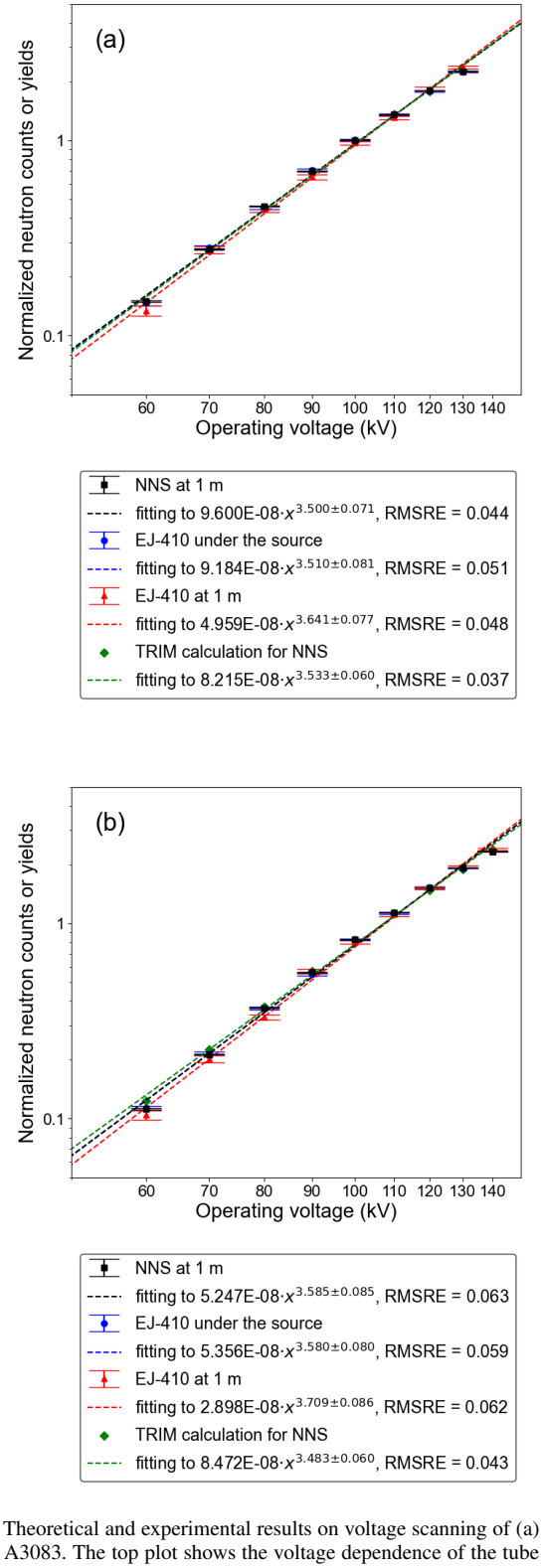

Fig. 3. Theoretical and experimental results on voltage scanning of (a) A3082 and (b) A3083. The top plot shows the voltage dependence of the tube A3082 while the bottom plot shows that of A3083 when both tubes were operated at the current of 70 μA. The neutron counts from measurements and the yield from TRIM calculations were normalized by their respective means for comparison. The root mean squared relative error (RMSRE) for each fitting is noted.

The maximum neutron emission from the A3082 was measured using the NNS surrounded by six shells, which have the highest neutron counts. Based on the MCNP6 calculation, taking into account of a factor of 1.03 between the measurement and calculation at shell 6 in Figure 4, at the current of 70 μA and voltage of 130 kV, the A3082 tube provided 4.7×10^8 n/s.

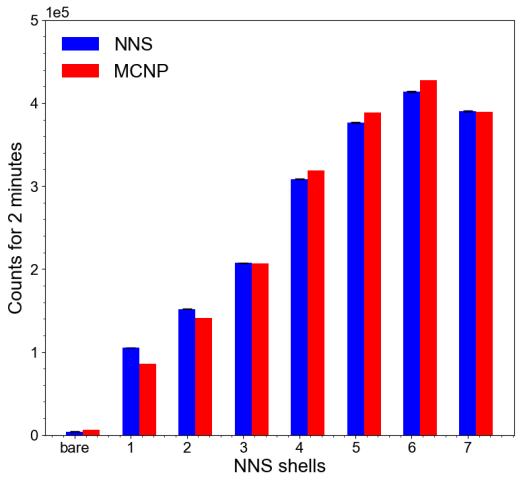

Fig. 4. Experiment (NNS) and theoretical (MCNP) ^{3}He neutron counts. Neutrons were measured for two minutes, for each shell configuration, at a 1 m distance from the source, A3083, at the current of 90 μA and voltage of 140 kV. MCNP results were scaled by the estimated source rate, 8.2×10^8 n/s. The statistical measurement errors are the square root of the number of counts, which are very small in this plot.

Another neutron detector, a BTI N-Probe, was used to cross check the results from the A3082. The BTI N-Probe was calibrated with a Cf-252 source, resulting in an uncertainty in dose rate of about 13% at the 95% confidence level. The calibration was performed using standards traceable to NIST. The N-Probe was located at a 3 m distance from the source with its maximum neutron yield. The flux above 6 MeV in the spectrum was 396 n/cm^2/s. Considering the detector distance from the source, an ideal calculation, ignoring the collimator and room, gives a source rate of 4.5×10^8 n/s. The full MCNP calculation gives a source rate of 4.6×10^8 n/s in order to match the neutron flux above 6 MeV from the experiment. This is easily within the mutual error range of the NNS measurement.

TRIM calculation gave 1.2×10^9 n/s for A3082 maximum neutron yield and 1.5×10^9 n/s for A3083. This is a factor of 2.6 (A3082) and 1.8 (A3083) greater than the yield measured in the experiments. This represents remarkably good agreement with a idealized first-principles calculation, given the approximate nature of the parameters of the system that could be provided by the manufacturer, the unknown sputtering erosion and damage to the target, as well as possible impurities, including ^{3}He, in the beam and the target.

C. *Effect of tritium decay*

Since we have two accelerator tubes, A3082 (8.44 years from the manufacture date) and A3083 (1.44 years), this might provide an opportunity to understand the temporal degradation of the neutron generator. One intuitive, but as we will see incorrect, assumption might be that the natural decay of the tritium could reduce tube performance. Tritium has a half-life of 12.3 years and decays to ^{3}He. We suppose that the target

is in equilibrium with the beam and the surrounding gas from which the beam is generated. Therefore, the tube would have the same ratio of deuterons to tritons in the beam and target.

The fraction in tritons in the beam and target t years after the date of manufacture, $f_T(t)$, can then be expressed as,

$$f_T(t) = \frac{f_T(t_0) \cdot e^{-\lambda t}}{f_T(t_0) \cdot e^{-\lambda t} + f_D(t_0)} = \frac{e^{-\lambda t}}{e^{-\lambda t} + 1} \qquad (2)$$

where $\lambda = \ln(2)/12.3$. We assume, as indicated by the manufacturer, there are equal numbers of deuterons and tritons in the gas when the generator is manufactured ($f_T(t_0) = f_D(t_0) = 0.5$). The deuteron fraction is simply $f_D(t) = 1 - f_T(t)$. We can have a generalized model by incorporating this temporal change to the current in Table I as shown in Table II. The calculation result of the fusion reaction rate at the voltage of 130 kV is shown in Figure 5.

TABLE II
ENERGY AND CURRENT OF BEAM PARTICLES WITH THE ACCELERATOR VOLTAGE $V_{\rm acc}$ AND CURRENT $I_{\rm acc}$ AFTER t YEARS FROM THE MANUFACTURE DATE.

Ion	Energy	Current
10% atomic beam		
D^+	$eV_{\rm acc}$	$0.1 f_D(t) I_{\rm acc}$
T^+	$eV_{\rm acc}$	$0.1 f_T(t) I_{\rm acc}$
90% molecular beam		
DD^+	$0.5eV_{\rm acc}$ (D)	$0.45 f_D(t) I_{\rm acc}$ (D)
	$0.5eV_{\rm acc}$ (D)	$0.45 f_D(t) I_{\rm acc}$ (D)
TT^+	$0.5eV_{\rm acc}$ (T)	$0.45 f_T(t) I_{\rm acc}$ (T)
	$0.5eV_{\rm acc}$ (T)	$0.45 f_T(t) I_{\rm acc}$ (T)
DT^+	$0.4eV_{\rm acc}$ (D)	$0.9 f_D(t) I_{\rm acc}$ (D)
	$0.6eV_{\rm acc}$ (T)	$0.9 f_T(t) I_{\rm acc}$ (T)

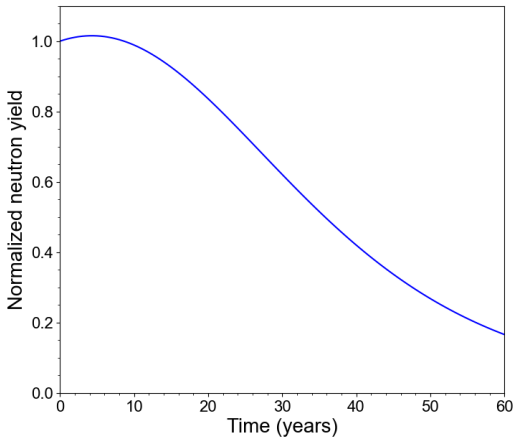

Fig. 5. Neutron yield at 70 μA and 130 kV over time. The yield is normalized by the yield at the date of manufacture.

Based on this calculation, we obtain a neutron yield slightly higher than its initial yield until 8.5 years, with a maximum around 4.5 years. At 10 years the the neutron yield is reduced from its original value by xyz%. While counter-intuitive compared with a naive estimation that the tube should lose performance proportional to its tritium depletion, this should not, in fact, be surprising. The factor $f_D f_T$ in the DT reaction rate does not change at first with tritium decay, but the relative velocity between the reactants immediately begins to increase. The beam will have the same total number of ions for the same total current, but due to tritium decay it will have a higher fraction of deuterons. Since the highest contributors to the neutron yield are D^+ and DD^+ striking tritium atoms in the target, a greater number of deuterons in the beam increases the D-T reaction rate. Eventually, the lower density of tritons in the target decreases the reaction rate.

At the time of the experiment, the A3083 was 1.44 years after the date of manufacture and the A3082 8.44 years. Based on the curve in Figure 5, the fusion rate of the A3083 increases by 0.85% and the A3082 by 0.13% from their initial state. The ratio between their two values is 1.0072. The experiment showed that the ratio of neutron counts at the voltage of 130 kV between the A3083 and A3082 was about 1.25. This difference does not, therefore, arise from tritium decay. Target degradation from titanium sputtering may have an important impact as well as the buildup of He over time. Based on the results presented here, these likely dominate over the direct effects of T decay.

V. CONCLUSIONS

In this study, we found the operating current and voltage dependence of the P385 neutron generator with A3082 and A3083 neutron tubes. We measured neutrons with a BTI N-Probe NE-213 liquid scintillator, a Detec Nested Neutron Spectrometer and two ZnS fast neutron scintillators. We modeled the neutron yield based on the TRIM code, which calculates the trajectory and the energy loss of deuterons and tritons within the target. Experimental and theoretical results both indicate linear dependence on the operating current. Experiments showed a 3.59 $\pm$0.08 power dependence on the voltage, consistent with the modeling prediction of 3.5. The two neutron detectors with traceable calibrations, the N-Probe and NNS, modeled with MCNP calculations showed that the A3083 and A3082 tubes give a maximum neutron yield of 8.2×10^8 n/s and 4.7×10^8 n/s, respectively, with $\pm$10% uncertainty. We showed that tubes such as these, at 1.44 and 8.44 years after manufacture, should be unaffected by tritium decay.

We consider that this study of the performance of the Thermo Scientific P385 neutron generator with two different neutron tubes will be of use to other users of this instrument. We have measured that the absolute yield is as specified by the manufacturer, we have provided a more accurate scaling with beam voltage than previously available for this system, and we have justified this result on the basis of TRIM modeling. We have also demonstrated that tritium decay is not a significant effect on performance over a period close even to the half-life of tritium.

ACKNOWLEDGMENT

We would like to thank Mr. James Simpson from Thermo Scientific for providing information about the Thermo Scientific P385 Neutron Generator and for comments on this paper, Dr. David Chichester from Idaho National Laboratory for sharing his unpublished work relevant to our study, and Dr. Valentin Fondement from University of Michigan for sharing

his expertise on a similar D-T neutron generator, the GENIE 16.

REFERENCES

[1] "Thermo Scientific P 385 Product Specifications," Thermo Fisher Scientific, Colorado Springs, CO, USA.

[2] R. Goldston, F. d'Errico, A. di Fulvio, A. Glaser, S. Philippe, and M. Walker, "Zero Knowledge Warhead Verification: System Requirements and Detector Technologies," presented at the *INMM Annual Meeting,* Atlanta GA, USA, July 20–24, 2014.

[3] Standard Test Method for Measuring Neutron Fluence and Average Energy from ^{3}H(d,n)^{4}He Neutron Generators by Radioactivation Techniques, ASTM E496-14, July 2022, 10.1520/E0496-14R22.

[4] R.H. Craig, "Calibration Of A 14 MeV Neutron Generator With Reference To NBS-1," in *AIP Conf. Proc.* 1 June 2011, 1336 (1), pp. 437–443. 10.1063/1.3586137.

[5] V. Fondement, B. Pérot, T. Marchais, J. Loridon, H. Toubon, Y. Bensedik, and J. Collot, "Electronics and 3He Counter Acquisition Tests During the Pulses of a D-T Neutron Generator," in *Proc. IEEE NSS/MIC,* Milano, Italy, 2022, pp. 1–6, 10.1109/NSS/MIC44845.2022.10399200.

[6] "Thermo Scientific P385 Neutron Generator Operation Manual," Thermo Fisher Scientific, Colorado Springs, CO, USA, Manual P/N 120006-A062907, 2010.

[7] J. Simpson, private communication, December 2023.

[8] J.F. Ziegler, M.D. Ziegler, M.D., and J.P. Biersak, "SRIM – The stopping and range of ions in matter (2010)," *NIM B*, vol. 268(11–12), pp. 1818–1823, June 2010, 10.1016/j.nimb.2010.02.091.

[9] M. Hepler, "Zero-knowledge Isotopic Discrimination for Nuclear Warhead Verification," Ph.D. disseration, Dept. Mech. Aero. Eng., Princeton Univ., Princeton, NJ, USA, 2020, pp. 67–70.

[10] H. Ing, S. Djeffal, T. Clifford, R. Machrafi, and R., Noulty, "Portable spectroscopic neutron probe," *Radiat. Prot. Dosimetry*, vol. 126(1–4), pp. 238–243, August 2007, 10.1093/rpd/ncm049.

[11] M. Koslowsky, "Spectral Unfolding: A Mathematical Perspective, Modern Neutron Detection," in *Proc. a Technical Meeting by IAEA,* Vienna, Austria, IAEA-TECDOC-1935, 2020, pp. 97–115.

[12] "Nested Neutron Spectrometer Operations, Data Acquisition and Data Analysis User Manual," ver. 2.1, Detec, Gatineau, QC, Canada.

[13] J. Dubeau, private communication, October 2024.

[14] G.F. Knoll, *Radiation of Detection and Measurement*, 4th ed., John Wiley & Sons, Inc., Hoboken, NJ, 2020, pp. 113–115.

[15] D.L. Chichester, E.H. Seabury, and A.J. Caffrey, "Measurement of the Neutron Yield of DD and DT Neutron Generators," presented at *2008 Symposium on Radiation Measurements and Applications*, Berkeley, CA, USA, June 2–5, 2008.

[16] C.J. Werner, J.S. Bull, C.J. Solomon, F.B. Brown, G.W. McKinney, M.E. Rising, D.A. Dixon, R.L. Martz, H.G. Hughes, L.J. Cox, A. J. Zukaitis, J.C. Armstrong, R. A. Forster, and L. Casswell, "MCNP6.2 Release Note", LANL, Los Alamos, NM, USA¡ Tech. Rep. LA-UR-18-20808, 2018.

[17] J. Simpson, private communication, May 2024.